



# Correcting Non-Uniform Beam Filling Effects for Spaceborne Weather Radars

Robert Meneghini, Code 612, NASA GSFC

Liang Liao, Goddard Earth Sciences & Tech Center / MSU

Non-uniform beam filling (NUBF) occurs when gradients in the radar reflectivity are present within the field of view (FOV) of the instrument. For example, in the case of the TRMM radar, the FOV is 5 km while convective cells can be as small as 1 km. This situation can lead to significant errors in the estimation of rain parameters. For off-nadir incidence angles, Takahashi et al. (2006) showed that multiple estimates of path integrated attenuation (PIA) can be made within the radar beam. Our work shows how these PIA estimates can be used to obtain attenuation-corrected radar reflectivities over the high-resolution columns within the beam (see Fig. 1). This provides a correction to the effects of non-uniform beam filling in the cross-track plane.

- Applying the method to a simple storm model shows that, in principle, the method provides accurate corrections to the non-uniform beam filling problem, if the path attenuations can be measured accurately.
- The method will be applied to data from the TRMM Precipitation Radar to assess its feasibility and accuracy.
- If successful, the method will be considered for application to the GPM dual-frequency Precipitation Radar.

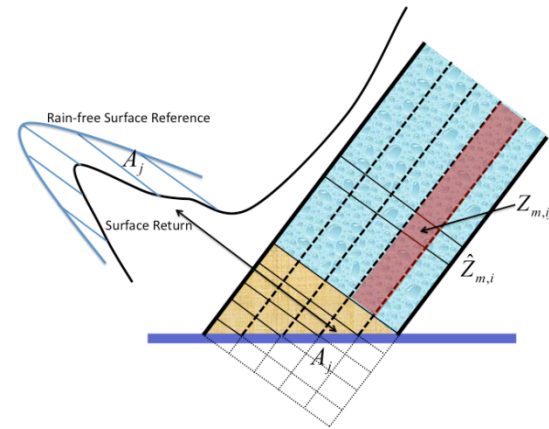


**Figure 1:** Schematic of the spaceborne radar geometry at an off-nadir incidence angle. The columns are defined by the range gates that intersect the surface. The path attenuation along each column is estimated by the difference between the radar surface returns outside and inside the rain.

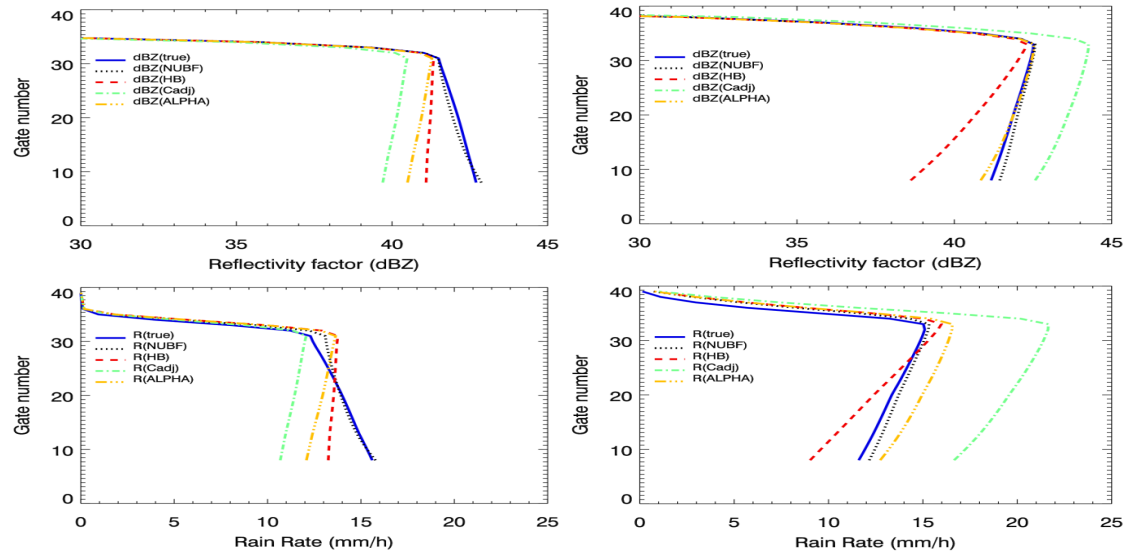


**Figure 2:** Examples of NUBF correction for the radar reflectivity factor ( $Z$ ), top panels, and rain rate ( $R$ ), bottom panels. True  $Z$  and  $R$  are given by the solid lines, the NUBF-corrected solutions by the dotted lines. Other curves show the results of several methods without an NUBF correction.



Name: Robert Meneghini, NASA/GSFC, Code 612

E-mail: robert.meneghini-1@nasa.gov

Phone: 301-614-5652

## References:

- Meneghini, R., L. Liao, S. Tanelli, and Stephen L. Durden, 2012: Assessment of the performance of a dual-frequency surface reference technique over ocean. *IEEE Transactions on Geoscience and Remote Sensing*, in press.
- Meneghini, R. and L. Liao, 2012: Modified Hitschfeld-Bordan equations for attenuation-corrected radar rain reflectivity: Application to non-uniform beam filling at off-nadir incidence, *Journal of Atmospheric and Oceanic Technology*, submitted.
- Durden S.L., S. Tanelli, and R. Meneghini, 2012: Using surface classification to improve surface reference technique over land, *Indian Journal of Radio & Space Physics*, **41**, 403-410.
- Meneghini, R., and J.A. Jones, 2011: Standard deviation of spatially averaged surface cross section data from the TRMM Precipitation Radar, *IEEE Geosciences and Remote Sensing Letters*, **8**, 293-297.
- Takahashi, N, H. Hanado, and T. Iguchi, 2006: Estimation of path-integrated attenuation and its non-uniformity from TRMM/PR range profile data. *IEEE Transactions on Geoscience and Remote Sensing*, **44**, 3276-3283.

## Technical Description of Figures:

**Figure 1:** Off –nadir cross-track radar geometry where the surface is represented by the blue horizontal line. The measured low-resolution radar reflectivity at range gate ‘i’ is denoted by  $\hat{Z}_{m,i}$  while the path integrated attenuation along the jth column is denoted by  $A_j$ . The high resolution ‘measured’ radar reflectivity at the intersection of the ith range and jth column is denoted by  $Z_{m,ij}$ . At left: determination of path attenuation,  $A_j$ , is illustrated as the difference in surface return powers along column j outside and inside the rain.

**Figure 2:** Low resolution estimates of Z and R, Z(NUBF) and R(NUBF), represented by the black dotted lines, are derived from the high resolution estimates of Z. True Z and R are represented by the solid blue lines. Also shown are the results from the low resolution standard Hitschfeld-Bordan, C-adjustment, and alpha-adjustment formulations. Left: results for a negative gradient in the cross-track dimension, x, where  $\text{dBZ}(x = -1) = 45$  and  $\text{dBZ}(x = 1) = 20$ . Right: results for a negative gradient in x where  $\text{dBZ}(x = -1) = 20$  and  $\text{dBZ}(x = 1) = 45$ .

**Scientific significance:** Effects of non-uniform beam filling can be a significant source of error in spaceborne weather radar retrievals of precipitation. The present method might mitigate these errors and lead to more accurate retrievals.

**Relevance for future science and relationship to Decadal Survey:** The method, if shown to be feasible, is applicable to any off-nadir airborne or spaceborne weather radar and therefore is relevant to present (TRMM PR) and future instruments (GPM DPR) of this type.



# Above-cloud absorbing aerosol effects and direct radiative forcing

Kerry Meyer, Steve Platnick, Lazaros Oreopoulos, and Dongmin Lee, Code 613, NASA GSFC

Aerosols remain a poorly constrained component of the Earth's atmosphere. Absorbing aerosols such as smoke strongly absorb solar radiation, particularly at ultraviolet and visible/near-infrared (VIS/NIR) wavelengths, and their presence above clouds can have considerable implications. In clear, cloud-free skies, aerosols have previously been shown to have a negative direct aerosol radiative forcing (DARF), i.e. a cooling effect, because they act primarily as a scattering layer. Absorbing aerosols overlying bright clouds, however, can have positive DARF, i.e. a warming effect, because their absorption is enhanced by increased reflection by the underlying clouds. This above-cloud absorption can also cause biases in estimates of the underlying cloud properties derived from satellite observations, specifically for passive retrieval techniques that rely on measurements of reflected solar radiation at VIS/NIR wavelengths. Moreover, biased cloud properties can yield biased estimates of the above-cloud DARF of absorbing aerosols, specifically because the cloud properties are a critical component in such calculations.

We focus on the southeast Atlantic Ocean during August and September, where smoke from extensive agricultural burning in Africa is persistently transported westward over low-altitude marine boundary layer clouds. Fig. 1 shows mean (a) cloud optical thickness (COT) and (b) effective particle radius ( $r_e$ ) obtained from the standard cloud retrievals of the Moderate-resolution Imaging Spectroradiometer (MODIS) on Aqua. We can estimate the strength of the above-cloud aerosol absorption using aerosol optical depth (AOD) from the Cloud-Aerosol Lidar with Orthogonal Polarization (CALIOP) on CALIPSO. Using this information to produce new unbiased MODIS cloud retrievals, we find that both mean COT and  $r_e$  increase as shown by the differences in Fig. 1 (c) and (d).

Using bias-adjusted cloud retrievals can yield better estimates of the above-cloud DARF of absorbing aerosols. Fig. 2 shows meridional mean instantaneous DARF, averaged over the domain in Fig. 1, using both standard (dashed lines) and bias-adjusted (solid lines) Aqua MODIS cloud retrievals (MYD06), as well as standard (black) and scaled (gray) CALIOP AOD (scaled to account for observed biases in the daytime CALIOP statistics with respect to the nighttime statistics). It is found that biased cloud retrievals yield smaller DARF estimates. This effect is illustrated by Fig. 3, which shows the above-cloud DARF of absorbing aerosols as a function of both COT and AOD. Here DARF is generally positive (warming), but decreases, even turning negative (cooling), as the underlying clouds become less bright (i.e., decreasing COT). Biased cloud retrievals, with smaller COT, thus can yield low-biased DARF estimates.

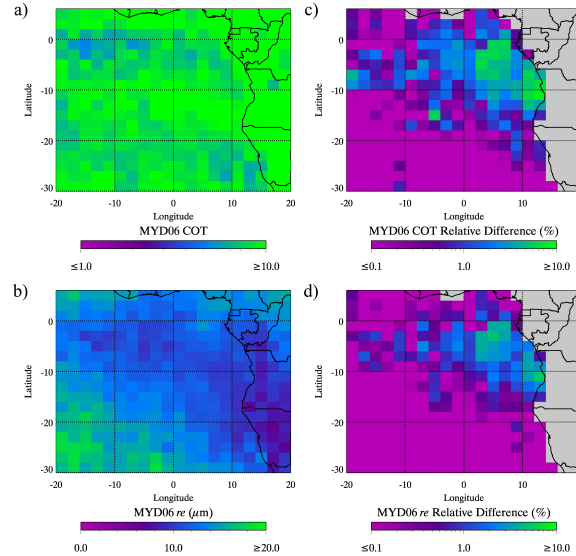


**Fig. 1.** MYD06 Collection 6 liquid cloud mean retrieved COT (a) and  $r_e$  (b) for pixels collocated with the CALIPSO ground track during August and September 2006-2011. Retrieval differences after adjusting for above-cloud aerosol absorption, averaged over all collocated ocean-only cloudy pixels, are shown for COT (c) and  $r_e$  (d).

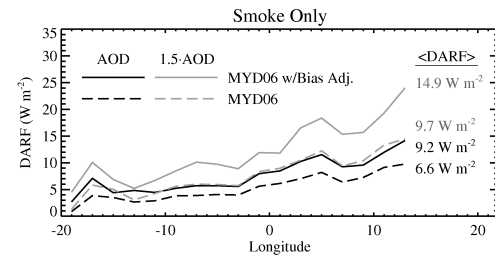


**Fig. 2.** Meridional mean above-cloud instantaneous DARF, averaged over the domain in Fig. 1, for smoke-polluted cloudy MODIS pixels only. Domain-averaged values ( $\langle \text{DARF} \rangle$ ) are also shown.

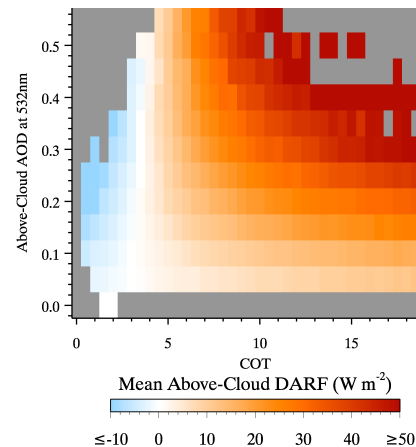


**Fig. 3.** Mean instantaneous above-cloud DARF, from the domain in Fig. 1, for smoke-polluted cloudy MODIS pixels as a function of both COT and above-cloud AOD. It is evident that underestimating COT, for instance as a result of VIS/NIR absorption by above-cloud smoke aerosols, can yield smaller DARF estimates.



Name: Kerry Meyer, Steve Platnick, Lazaros Oreopoulos, and Dongmin Lee, NASA/GSFC, Code 613

E-mail: [kerry.meyer@nasa.gov](mailto:kerry.meyer@nasa.gov)

Phone: 301-614-6186

### References:

Meyer, K., S. Platnick, L. Oreopoulos, and D. Lee (2012), Estimating the direct radiative forcing of absorbing aerosols overlying marine boundary layer clouds in the southeast Atlantic using MODIS and CALIOP, *J. Geophys. Res.*, submitted.

### Data Sources:

Aqua MODIS Level-2 cloud product (MYD06), CALIOP Level-2 5km aerosol layer product, NCEP GDAS model re-analyses.

### Technical Description of Figures:

**Figure 1:** MYD06 Collection 6 liquid cloud mean retrieved COT (a) and  $r_c$  (b) for pixels collocated with the CALIPSO ground track during August and September 2006-2011 aggregated to a  $2^\circ$  grid. Retrieval differences after adjusting for above-cloud aerosol absorption, averaged over all collocated ocean-only cloudy pixels, are shown for COT (c) and  $r_c$  (d). Because the retrieval adjustment is only performed over the ocean, grid boxes in which the surface is predominantly land are shaded gray in (c) and (d).

**Figure 2:** Meridional mean instantaneous (i.e., at the time of observation) above-cloud DARF, averaged over the six-year CALIOP/MODIS collocated data record (August/September 2006-2011), for cloudy MODIS pixels for which CALIOP produces reliable above-cloud smoke subtype aerosol retrievals (i.e., only the polluted cloudy pixels). The solid and dashed lines denote TOA DARF using the bias-adjusted and non-adjusted MYD06, respectively; the black and gray lines denote the use of CALIOP-derived above-cloud AOD and scaled AOD ( $\times 1.5$ ), respectively. Mean DARF for each case ( $\langle \text{DARF} \rangle$ ), averaged over the entire domain ( $30^\circ\text{S}$  to  $6^\circ\text{N}$ ,  $20^\circ\text{W}$  to  $30^\circ\text{E}$ ), is shown at the right of each plot. The DARF values shown here are derived from solar broadband radiative transfer (RT) calculations using the RRTMG-SW RT code.

**Figure 3:** Mean instantaneous (i.e., at time of observation) above-cloud DARF for cloudy MODIS pixels for which CALIOP produces reliable above-cloud smoke subtype aerosol retrievals, as a function of both COT and above-cloud AOD.

**Scientific Significance:** Because aerosols are an as yet unconstrained component of the Earth's atmosphere, they have been the focus of significant recent research. The presence of absorbing aerosols above clouds can have considerable implications because they strongly absorb solar radiation at ultraviolet and visible/near-infrared (VIS/NIR) wavelengths. This can be problematic for satellite remote sensing retrievals of the underlying cloud optical properties, particularly those techniques that rely on VIS/NIR reflectance measurements. Such reflectance measurements have been shown, both here and by previous studies, to be biased by the above-cloud aerosol absorption. Furthermore, estimates of the radiative impacts of the above-cloud aerosols themselves may be biased as a result of biased cloud retrievals. It is thus important to understand these radiative effects and to provide accurate, un-biased retrievals of both the cloud and aerosol properties.

**Relevance for future science and relationship to Decadal Survey:** Our understanding of the radiative effects of aerosols, particularly above clouds where remote sensing retrievals are difficult to obtain, needs to be improved. As shown here, combining multiple A-Train sensors provides an opportunity to enhance our ability to resolve this issue.



# Well-Calibrated Ground Stations Help Mitigate against Upcoming Gap in Global Ozone Profile Measurements



Thomas J McGee, Code 614; L Twigg (SSAI); G Sumnicht (SSAI), and D Swart, (RIVM)

ozone anomalies, ~40 km (2 hPa), 60°S to 60°N

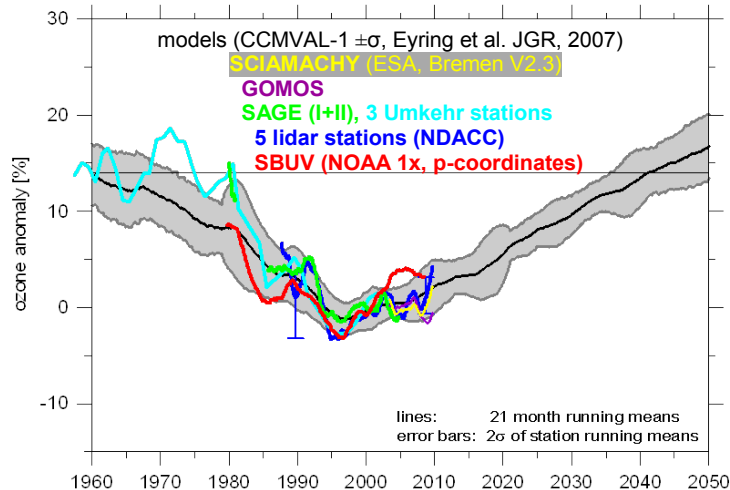


**Figure 1:** The plot shows calculated (model data) and satellite measured per cent changes in ozone at 2 hPa (near 40 km). The satellite data are averaged between 60°S and 60°N. Superimposed on this model data are data from 3 ground-based Umkehr stations (light blue) and five NDACC lidar stations (blue) which show very good agreement with the satellite data.

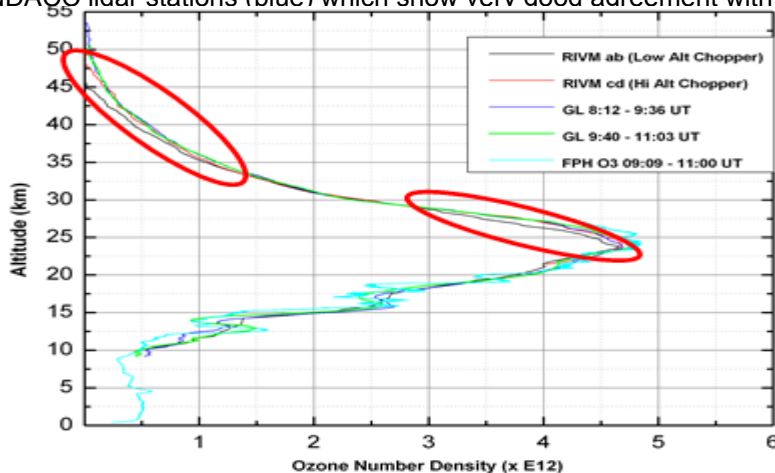


**Figure 2.** The red ovals indicate differences from the GSFC lidar noted in the new data protocol used to acquire the RIVM ozone profiles. The new configuration leads to biases between 23-30 km and above ~ 35 km. The new protocols need to be modified.

Recent work (Steinbrecht et al., 2009) has illustrated the capability for a few well-calibrated ground-based stations making frequent measurements, to reproduce the long-term global behavior in both ozone and temperature as measured by satellite instrumentation (see Figure 1). This plot is based on global data from SCIAMACHY, GOMOS, SAGE (I and II), as well as ground-based Umkehr measurements, and lidar measurements at five NDACC stations. The solid horizontal line in the figure represents 1960 ozone levels. This ability is especially important with a looming gap in satellite measured ozone profiles.

Goddard scientists have developed a mobile, ground-based lidar instrument for the validation of NDACC lidar instrumentation at NDACC sites around the world (McGee, 1995). The Stratospheric Ozone (STROZ) Lidar makes simultaneous measurements of ozone, temperature, aerosol and water vapor profiles. This lidar, as part of the NDACC Validation Protocol has validated all five of the stations used in the Steinbrecht study, (four of them multiple times).

The Lauder, NZ lidar, operated by RIVM of the Netherlands, recently made significant changes in its' data acquisition system to acquire simultaneous low altitude and upper altitude ozone data. These changes induced biases in the RIVM data which were detected by the GSFC lidar (Fig.2, red ovals). Results indicated that instrumental changes are required, or a return to the previous data acquisition protocol is necessary to avoid the errors.



Name: Thomas J. McGee, NASA/GSFC, Code 614  
E-mail: thomas.j.mcgee@nasa.gov  
Phone: 301-614-5980



## References:

Steinbrecht, W., H. Claude, F. Schonenborn, I. S. McDermid, T. Leblanc, S. Godin-Beekmann, P. Keckhut, A. Hauchecorne, J. A. E. Van Gijssel, D. P. J. Swart, G. E. Bodeker, A. Parrish, Ozone and temperature trends in the upper stratosphere at five stations of the Network for the Detection of Atmospheric Composition Change, *International Journal of Remote Sensing*, vol. 30, no. 15, pp. 3875-3886, 2009.

McGee, T. J., M. Gross, U. N. Singh, J. J. Butler, and P. E. Kimvilakani, Improved stratospheric ozone lidar, *Optical Engineering*, 34, 1421-1430, 1995.

**Data Sources:** Data presented in both figures are publically available from the NDACC data archive. Additional ancillary data for Figure 2 are available from the GSFC POC.

## Technical Description of Figures:

**Figure 1:** shows a comparison of available long term ozone data at 40km, averaged between 60S and 60N. The x-axis shows monthly ozone anomalies, i.e., the change in the monthly mean compared to the monthly average over the years 1998 – 2007. These years were chosen because ozone values were relatively constant. The measurements show a steady decline in ozone from 1960, bottoming out near 2000, and followed by a slow recovery. A significant point to be taken from these data is that the data from a limited set of ground-based, well-calibrated instruments shows the same behavior as global satellite data, with much less latitudinal and longitudinal coverage. The Goddard lidar instrumentation has played an ongoing role in the validation of these NDACC instruments.

**Figure 2:** The Lauder/RIVM lidar made changes in its data acquisition approach which necessitated increasing the intensity of the lidar return on its' detectors. This increase in signal level has induced non-linearities (noted in the red ovals in the Figure) in the detectors which lead to biases in the retrieved ozone profile data product. Comparison with the GSFC validation standard lidar points out these differences, and additional, joint experiments helped to clarify the results. Conclusions drawn from these measurements require further hardware changes or a return to the previous data acquisition protocol.

**Scientific significance:** The importance comes from the fact that high quality measurements require periodic and ongoing validation if long-term changes are to be detected. The Goddard lidar has provided an important, and independent way to tie ozone and temperature profile measurements together across a large quasi-global network. This is especially important since the work of Steinbrecht shows that in the absence of global satellite profile measurements, ground-based ozone profiles can proved a way to maintain the long-term data record, provided the instruments are validated periodically, particularly after instrumental changes.

**Relevance for future science and relationship to Decadal Survey:** Continued high quality measurements of ozone profiles are needed to adequately follow the recovery of stratospheric ozone. The only NASA Decadal Survey Mission which might make such global measurements in the future is the tier 3 mission, GACM.

**Acronyms:** NDACC – Network for the Detection of Atmospheric Composition Change; GOMOS - Global Ozone Monitoring by Occultation of Stars; CCMVal - Chemistry Climate Model Validation Activity; SCIAMACHY - Scanning Imaging Absorption Spectrometer for Atmospheric Chartography; SAGE - Stratospheric Aerosol and Gas Experiments; HALOE - Halogen Occultation Experiment; SBUV – Solar Backscatter Ultra-Violet Instrument